Proc. 4th Int. Symp. on Smart Control of Turbulence,
Tokyo, March 2-4, 2003

Evaluation of a GA-based Feedback Control System with Arrayed Micro Sensors and Actuators in a Turbulent Channel Flow

Yuji SUZUKI, Takashi YOSHINO, and Nobuhide KASAGI
Department of Mechanical Engineering, The University of Tokyo,
Hongo 7-3-1, Bunkyo-ku, Tokyo, 113-8656, Japan.
e-mai: ysuzuki@thtlab.t.u-tokyo.ac.jp

A prototype system for feedback control of wall turbulence is developed, and its performance is evaluated in a physical experiment. Arrayed micro hot-film sensors with a spanwise spacing of 1 mm are employed for the measurement of streamwise shear stress fluctuations, while arrayed magnetic actuators having 3 mm in spanwise width are used to introduce control input through wall deformation. The frequency response of the sensors and actuators is found to be sufficiently high for the flow conditions presently considered. A digital signal processor having a time delay of 1.6 ms is employed to drive output voltage for actuators. Feedback control experiments are made in a turbulent air channel flow using a genetic algorithms-based optimal control scheme. It is found that the wall shear stress fluctuation is decreased by up to 6% among 1000 trials in 100 generations. Second generation feedback control system using 192 sensors and 48 actuators is under development. Attempts to develop sensors having higher response and wall deformation actuators with MEMS technology are also discussed.

1. INTRODUCTION

In the last decade, feedback control of wall turbulence was extensively pursued because of its potential of high control performance with small energy input [1-3]. In such a control system, the near-wall coherent structures, which are responsible for regeneration cycle of turbulence, should be detected by sensors mounted on the wall, and selectively manipulated by the motion of actuators. Although the coherent structures have generally very small spatio-temporal scales, recent development of microelectromechanical systems (MEMS) technology has made it possible to fabricate flow sensors and mechanical actuators of submillimeter scale [4].

Recently, Endo et al.[5] carried out direct numerical simulation (DNS) of turbulent channel flow, in which arrayed wall shear stress sensors and wall-deformation actuators of finite spatial dimensions are assumed. They developed a practical control algorithm based on physical arguments on the near-wall coherent structures, and found that drag reduction of 12 % can be achieved by attenuating the near-wall streamwise vortices. Morimoto et al. [6] employed genetic algorithms in order to develop a simple feedback scheme based on the streamwise wall shear stress fluctuations. They obtained drag reduction of 12 % by using local wall blowing/suction. These findings encourage us to develop a feedback control system using distributed micro sensors and actuators as shown in Fig. 1.

The objectives of the present study are to develop a prototype of feedback control system with arrayed micro hot-film shear stress sensors and wall-deformation magnetic actuators, and to evaluate its performance in a turbulent air channel flow.

2. PROTOTYPE FEEDBACK CONTROL SYSTEM OF TURBULENT CHANNEL FLOW

2.1 Roadmap of feedback control system

Figure 2 shows the roadmap of our feedback control system in the University of Tokyo. In 2001, we developed an early prototype of the feedback control system using hot-film wall shear stress sensors and magnetic wall-deformation actuators. Turbulent velocity field above the actuator was measured with the aid of two-component LDV, while simple feedback rule was applied. It is found that the actuator can introduce wall-normal velocity fluctuations of about $v_{rms}=0.8u_\tau$ in the flow field, which should be large enough for controlling near-wall coherent structures[7].

In 2002-2003, the first-generation feedback control system having 24 hot-film shear stress sensors, and 4 miniature magnetic wall-deformation actuators is built[8]. A GA-based control algorithm is applied and the performance of the system is evaluated in a turbulent channel flow. We also develop key technologies for arrayed MEMS sensors and actuators such as optimal design of hot-film shear stress sensor, and backside electrical contact as described in Chap. 3.

Number of arrayed sensors and actuators is increased rapidly, and the third generation system will have about 250 arrayed sensors and actuators. DSP controller will be replace with a FPGA system, which has much smaller time delay in the control loop. Integrated driving circuits of the sensors and the feedback controller will also be realized on an analog VLSI chip. In 2004, the third generation fully-integrated system, which consists of hot-film sensors having backside contact, MEMS wall-deformation actuators, and analog VLSI controllers will be developed. Practical control algorithms based on suboptimal control theory is also under development with the aid of DNS, while GA-based schemes is applied first.

Figure 3a shows contours of two-point correlation of blowing/suction control input on the wall in the DNS study of Morimoto et al.[6]. The region of high correlation coefficient is confined in the area of $-20<\Delta z^+<20$ and $-100<\Delta x^+<100$. Those dimensions are in accordance with the DNS result of Endo et al.[5], where typical length scales of the wall deformation is elongated in the streamwise direction. Thus, the spanwise and streamwise lengths of the actuator should be respectively smaller than 40 and 200 viscous units.

Figure 3b shows the time spectra of v_w, wall shear stress fluctuations t_w and cross spectra of v_w and τ'_w [6]. The spectra of v_w and τ'_w suddenly drop at $f^+=0.1$. Therefore, the requirement for the time scale of sensors and actuators is $f^+=0.1$, which corresponds to about 300Hz at $Re_\tau=300$. On the other hand, the cross spectra of v_w and τ'_w is decreased with increasing frequency from $f^+=0.02$. Therefore, wall shear stress fluctuations at $f^+>0.02$ have less contribution to the control input, and the requirement for the time scale of the sensor is somewhat eased.

2.2 First generation feedback control system

Figure 4 shows a prototype control system, which consists of three rows of 8 hot-film shear stress sensors with a spanwise spacing of 1 mm and two rows of arrayed wall-deformation actuators in between with a 4.3 mm spacing. The spanwise spacings of the sensors and actuators are respectively about 14 and 60 wall units under the flow condition described later. The last row of the sensors is employed to evaluate the cost function described below.

Magnified view and schematic of the cross section of the shear stress sensor is shown in Fig. 4. A platinum hot-film is deposited on a SiN_X diaphragm (400×400 μm^2) of 1 μm in thickness, and a 200 μm-deep air cavity is formed underneath. Yoshino et al.[9] found that the frequency response of this first generation sensor (Type 1) is low, and the gain is deteriorated at f>40Hz. On the other hand, the spanwise

two-point correlation of τ'_w measured with the arrayed sensors exhibits a negative peak at $\Delta z^+ \sim 50$, and is in good accordance with the DNS data [10] (Fig. 5). Therefore, the near-wall coherent structures, which are the target of the feedback control, can be well captured with the present wall shear stress sensors.

For the wall-deformation magnetic actuator, a silicone rubber sheet of 0.1 mm in thickness is used as an elastic membrane, and 4 pairs of a rare-earth miniature permanent magnet of 1 mm in diameter and a miniature copper coil of 3 mm in diameter are used to drive one actuator elongated in the streamwise direction. Since the wall displacement is a nonlinear function of the voltage applied, the dynamic response of the actuator also depends on the driving voltage. The resonant frequency is 600 Hz for 4 *Vp-p* signal with a maximum amplitude of 0.25mm, which satisfies the requirement for Re_τ=300 as described above.

A digital signal processor (DSP) board (SMT-326, Sundance DSP Inc.) with 32 analog input/output channels is used as the controller of the present system. The output voltage of the constant temperature circuits for the hot-film sensors are firstly digitized with 16 bit AD converters. The control signals for the actuators are then computed with the DSP (C44, 60MFLOPS) and converted back to analog signals using 16 bit DA converters. The present DSP system has an inherent time delay of 1.6 ms due to internal data transfer and processing. The time delay of the feedback control loop is found to be 2.2 ms [7].

A turbulent air channel flow facility is employed for evaluating the present feedback control system. The cross section of the channel is 50×500 mm^2, and the test section is located 4 m downstream from the inlet, where the flow is fully-developed. The control system is placed at the bottom wall of the test section. The bulk mean velocity U_m is varied from 2.5 to 9.3 m/s, which corresponds to the Reynolds number Re_τ based on the wall friction velocity u_τ and the channel half-width from 250 to 800. When Re_τ=300 (U_m=3.0 m/s), one viscous wall and time unit correspond to 0.09 mm and 0.5 ms, respectively. At this flow condition, the mean diameter of the near-wall streamwise vortices is estimated to be 2.7 mm, while its characteristic time scale is 7.5 ms.

2.3 Genetic algorithm-based feedback control

An optimal control scheme based on genetic algorithm (GA) is employed in the present experiment. Driving voltage of each wall-deformation actuator E_A is determined with a linear combination of the streamwise wall shear stress fluctuations $\tau_w'_i$, i.e.,

$$E_A = \sum_{i=1}^{3} C_i \cdot \tau_w{}'_i \tag{1}$$

where $\tau_w'_i$ is measured with three sensors located upstream. The control variables C_i are optimized in such a way that a cost function based on the wall shear stress fluctuation given by

$$J = \int_t^{t+\Delta T} \tau_w{}'^2 \, dt \tag{2}$$

is minimized. The quantity C_i is expressed with a binary-coded string with 5 bits, which corresponds to a gene, and *N* individuals including a set of genes are made. Feedback control experiment using each individual, i.e., different set of C_is is independently carried out, and the cost function is calculated on line. Then, individual having smaller cost is statistically selected as parents, and two offsprings are made through crossover operation between them [6]. In total, *N* children are created by applying the crossover operation *N*/2 times. Finally, mutations at a given rate is applied to all genes of the *N* individuals. New generations are successively produced by repeating this procedure. Optimal solution is obtained when

the evolution is found to be in convergence. The population size N and number of generation are respectively chosen as 10 and 100, so that 1000 trials with different set of control variables are made in total. The integration time ΔT is chosen as 40 s (ΔT^+=8000). Note that no failure in the control system was observed during experiments, although total time for the optimization is more than 11 hours (on the order of 10 million cycle motion for the actuators).

Figure 7 shows the root-mean-square value of the wall shear stress fluctuations versus generation of the GA-based algorithms. Whereas there exists a large scatter among trials with different genes, 6% reduction is obtained at Generation 100. This fact encourages us to build the second generation system with massive arrayed sensors and actuators.

3. TOWARD FULLY-INTEGRATED FEEDBACK CONTROL SYSTEM WITH MASSIVE ARRAYED SENSORS AND ACTUATORS

3.1 Improvement of frequency response for wall shear stress measurement

It is well know that heat conduction loss to the substrate deteriorates the frequency response of thermal sensors[11], but the reason for the insufficient response of the hot-film sensor equipped with insulation air cavity remains unclear. Numerical simulation of the thermal field around the hot-film sensor was carried out, In order to improve its frequency response. Figure 8 shows the two-dimensional computational model. The fluid velocity was given as a linear function of the distance to the wall in order to mimic the fluctuating fluid velocity near the wall. Prandtl number Pr (=ν/α) is equal to 0.7 which corresponds to air.

Figure 9a shows the temperature distribution around sensor model with adiabatic wall, where heat loss to the substrate is assumed to be zero. It is found that thermal field spreads out in fluid even in the upstream direction due to the heat conduction. This high-temperature region surrounding the hot-film inhibits exposure of fluid at ambient temperature to the hot-film, and thus the gain of this sensor model is decreased with increasing frequency. Therefore, heat conduction in fluid significantly affects the response of the sensor

We also numerically examined the response of the sensor models having slit on the both sides of the hot-film and different length of the SiN_x diaphragm. Since thermal conductivity of air is orders of magnitude smaller than that of SiN_x, the slits inhibit tangential heat conduction in the diaphragm. As shown in Fig. 9b, the extent of the high-temperature region is confined by the slits when the cavity length W is 200μm, and the hot-film is closer to the ambient-temperature fluid than in Fig. 9a. Although it is not shown here, the frequency response is increased with decreasing W, and W becomes optimum at W=200~300 μm. The frequency response for W=200~300 μm is higher than the 'ideal' sensor with adiabatic wall [12].

Figure 10 shows our second-generation sensor based on the numerical results described above (Type 2). The length of the diaphragm is chosen as 200 μm. As shown in Fig. 11, the frequency response of Type 2 is remarkably improved over that of Type 1, and its power spectrum is in good agreement with the DNS data [10]. The cutoff frequency where the gain becomes 50% of the DNS data is increased from 70Hz to 400Hz. The root-mean-square vale of the streamwise wall shear stress $\tau_{w\,rms}$ normalized by its mean value $\tau_{w\,mean}$ is about 0.36 and good agreement with DNS data [10] at Re_τ<400.

Attempt to fabricate wall shear stress sensors having backside electronic contact is also made using novel feed through MEMS technology. Arrayed backside contact sensor with 1mm spanwise spacing is now under development.

3.2 Arrayed magnetic wall-deformation actuators

Figure 12 shows magnetic wall-deformation actuators having 2.4mm in width and 14.2mm in length. Spanwise spacing is 3.2mm, and 16 actuators are located in a spanwise length of 48mm. The maximum amplitude and the resonant frequency are respectively estimated to be 0.1mm and 400Hz, respectively. These actuators are designed for our second generation control system as shown in Fig. 13. MEMS magnetic actuators using thin-film electrodes and CVD-deposited polymer film are also under development for our third generation system.

CONCLUSIONS

The prototype of the feedback control system for wall turbulence is developed with arrayed micro hot-film sensors and arrayed magnetic wall-deformation actuators. The dynamic response of the sensors and actuators are found to be sufficiently high for the experimental condition employed. Genetic algorithm-based control scheme is applied to feedback control of a turbulent channel flow, and driving voltage of the actuators is assumed to be a linear combination of the wall shear stress fluctuations measured at three locations upstream. Control variables are optimized in such a way that the time integral of the wall shear stress fluctuations is minimized. It is found that the root-mean-square value of the wall shear stress is decreased by 6% among 1000 trials in 100 generations. Sensors having improved frequency response and backside electrical feed through are developed. Magnetic actuators for massive arrayed control system are also under development.

The authors are grateful to Messrs. S. Kamiunten and N. Zushi in Yamatake Corp. for his corporation in manufacturing micro shear stress sensors.

REFERENCES

[1] Moin, P., and Bewley, T., Appl. Mech. Rev., Vol. 47, (1994), pp. S3-S13.
[2] Gad-el-hak, M., Appl. Mech. Rev., Vol. 49, (1996), pp. 365-379.
[3] Kasagi, N., Int. J. Heat & Fluid Flow, Vol. 19, (1998), pp. 128-134.
[4] Ho, C.-M., and Tai, Y.-C., ASME J. Fluids Eng. Vol. 118, (1996), pp. 437-447.
[5] Endo, T., Kasagi, N., and Suzuki, Y., Int. J. Heat & Fluid Flow, Vol. 21, (2000), pp. 568-575.
[6] Morimoto, S., Iwamoto, K., Suzuki, Y., and Kasagi, N., Bull. Am. Phys. Soc., Vol. 46, (2001), p. 185.
[7] Yoshino, T., Suzuki, Y., and Kasagi, N., Proc. 5th JSME-KSME Fluids Eng. Conf., Nagoya, (2002), CD-ROM, OS4-1.
[8] Yoshino, T., Suzuki, Y., and Kasagi, N., Proc. 3rd Symp. on Smart Control of Turbulence, Tokyo, (2002), pp. 115-120.
[9] Yoshino, Y., Suzuki, Y., Kasagi, N., and Kamiunten, S., 2nd Int. Symp. Turbulence and Shear Flow Phenomena, Stockholm, Vol. II, (2001), pp. 153-158.
[10] Iwamoto, K., Suzuki, Y., and Kasagi, N., Int. J. Heat & Fluid Flow, Vol. 23, (2002), pp. 678-689.
[11] P. H. Alfredsson, A. V. Johansson, J. H. Haritonidis, and H. Eckelmann, Phys. Fluids, vol. 31, no. 5, (1988), pp. 1026-1033.
[12] T. Yoshino, Y. Suzuki, N. Kasagi, and S. Kamiunten, Proc. IEEE Int. Conf. MEMS 2003, Kyoto, (2003), pp. 193-196.

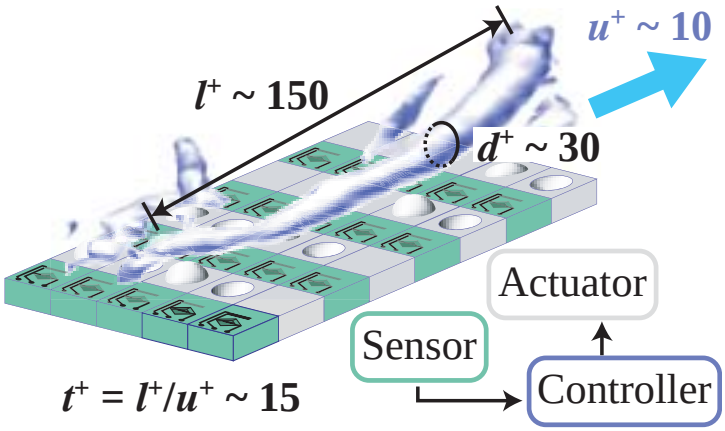

Fig. 1 Schematic diagram of active feedback control system for wall turbulence.

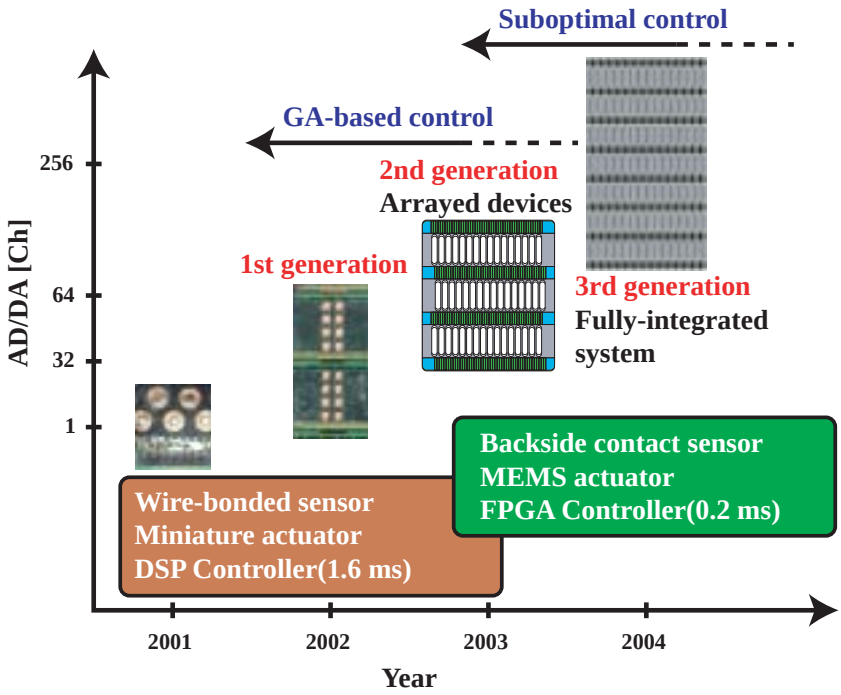

Fig. 2 Roadmap of feedback control system of wall turbulence in the University of Tokyo.

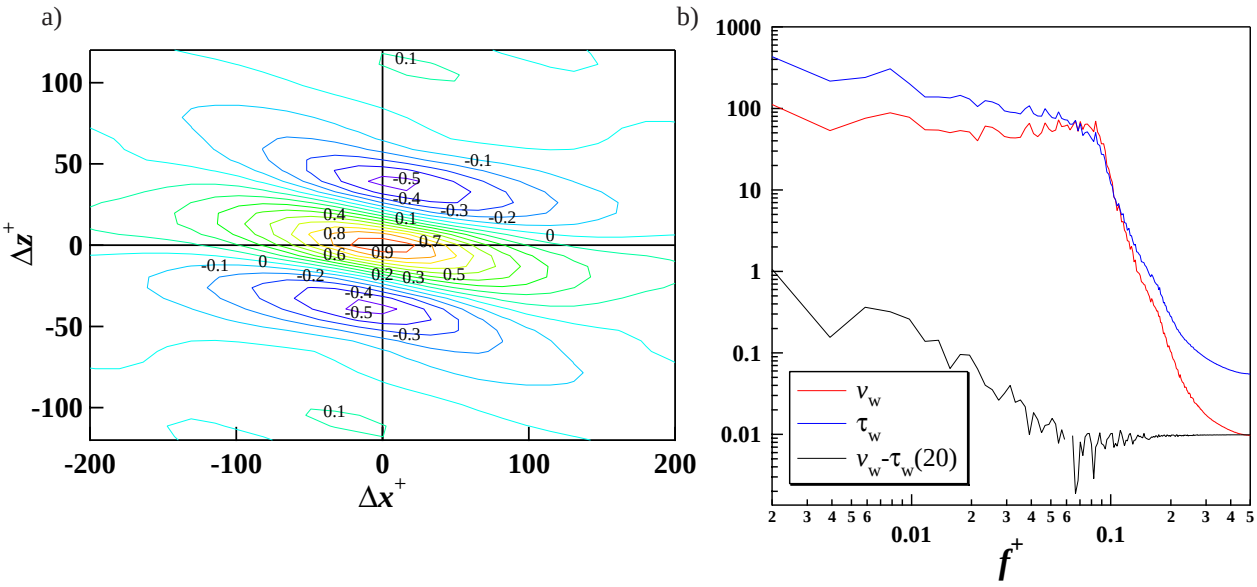

Fig. 3 DNS results of GA-based feedback control of turbulent channel flow (Morimoto et al., 2001). a) Contours of two-point correlation of the blowing/suction control input. b) Time spectra of blowing/suction control input v_w, wall shear stress fluctuations τ_w and cross spectra ofv_w and τ_w.

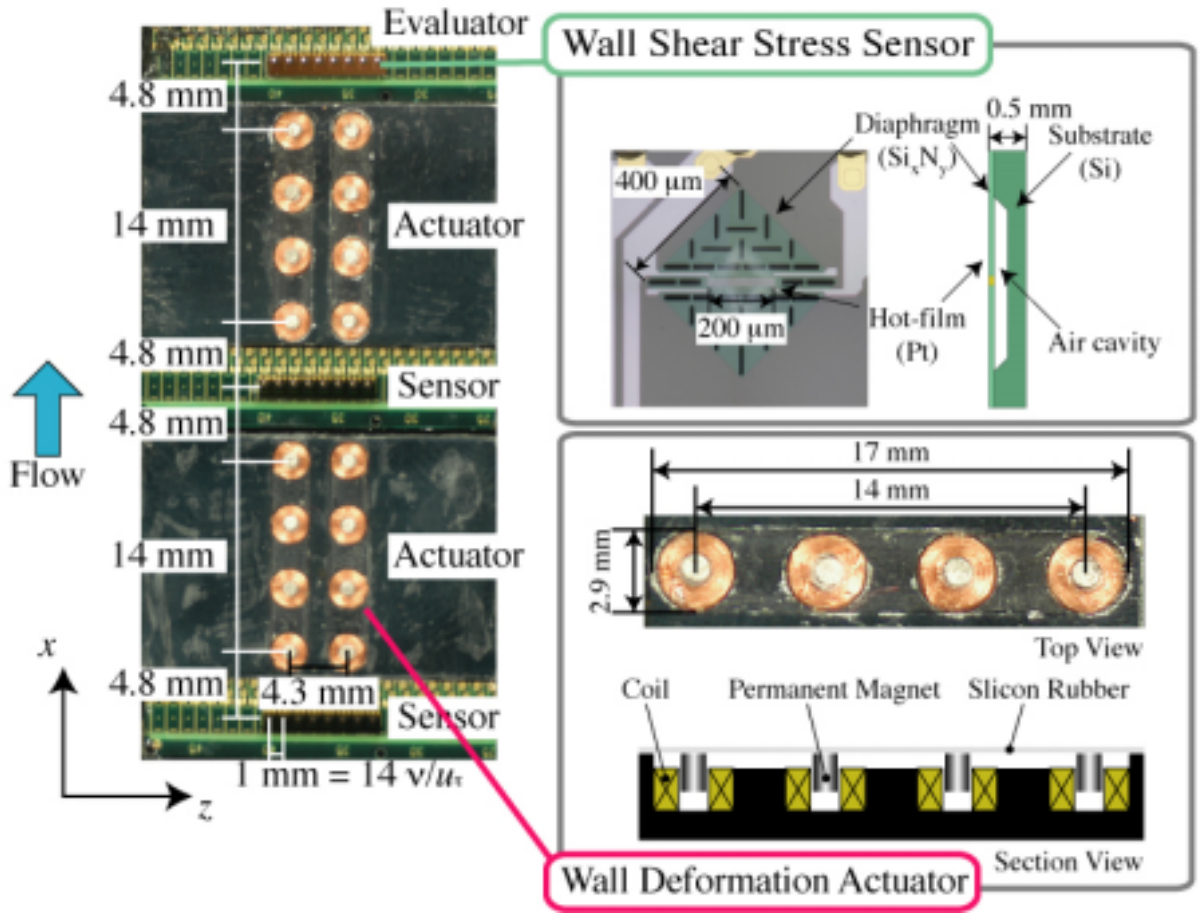

Fig. 4 First generation feedback control system of turbulent channel flow using 24 wall shear stress sensors and 4 wall deformation actuators.

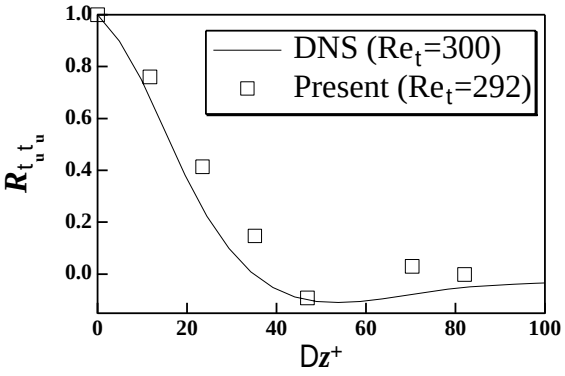

Fig. 5 Spanwise two-point correlation coefficients of the streamwise wall shear stress fluctuations.

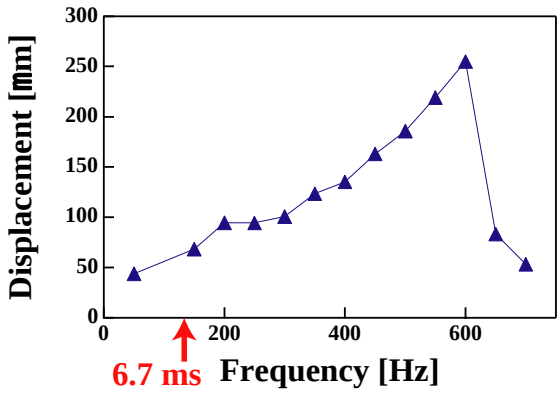

Fig. 6 Dynamic response of magnetic wall deformation actuator.

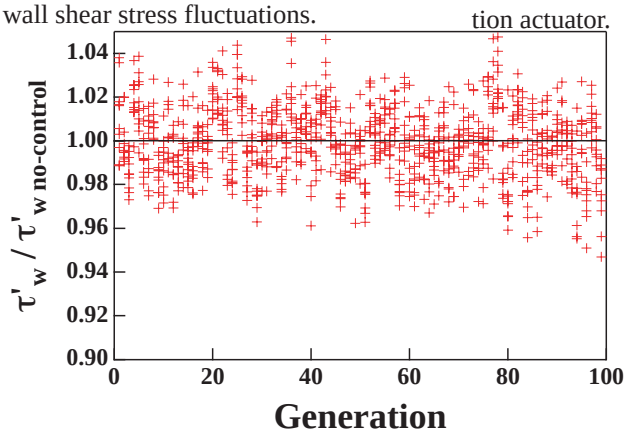

Fig. 7 Feedback control results using the 1st generation control system. Root-mean-square value of the wall shear stress fluctuations is plotted versus generation of GA-based control algorithm.

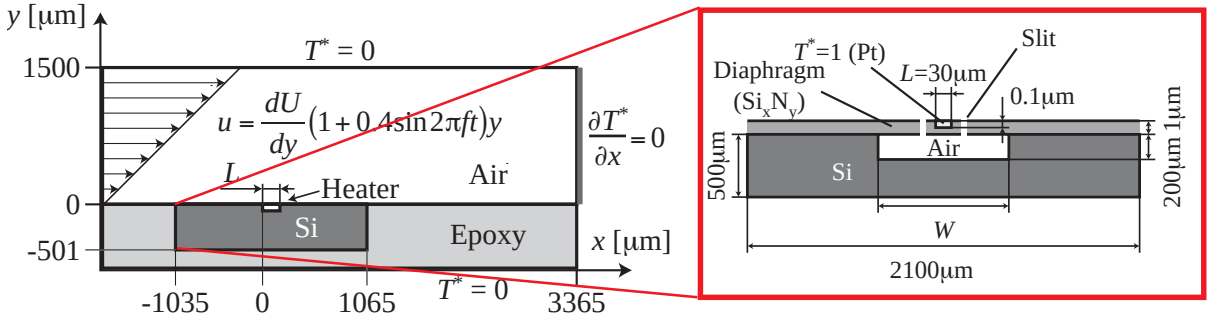

Fig. 8 Computational domain and schematic of sensor model.

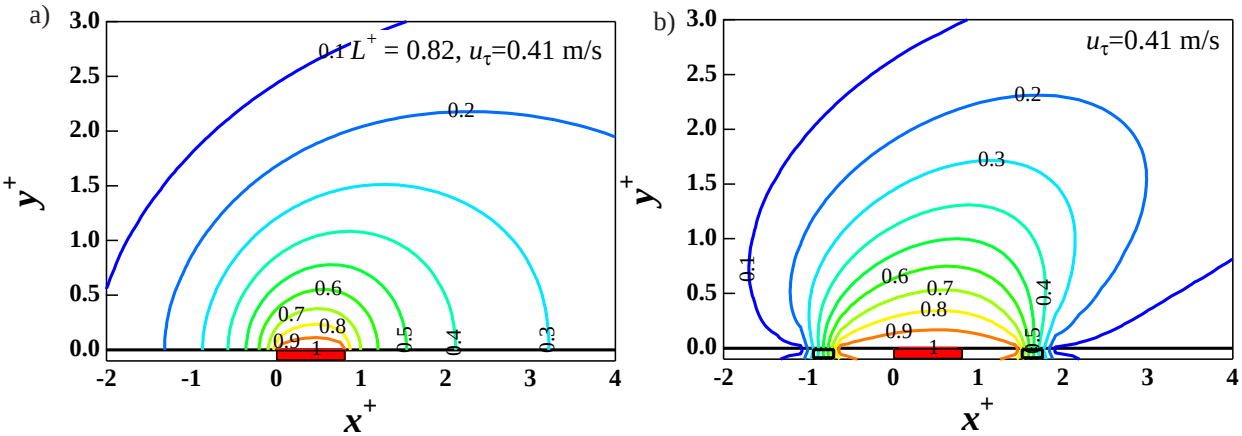

Fig. 9 Temperature distribution around the hot-film. a) Sensor model with adiabatic wall, b) Sensor model having diaphragm (W=200μm) with slit on the both side of the hot-film.

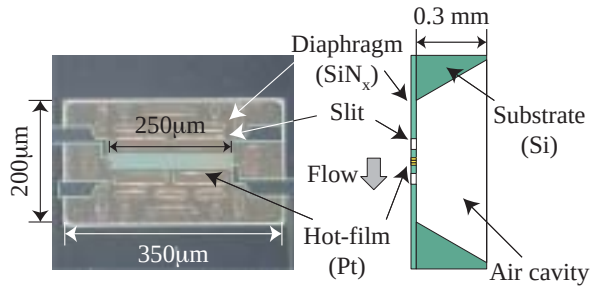

Fig. 10 Magnified view of micro hot-film shear stress sensor presently developed (Type 2).

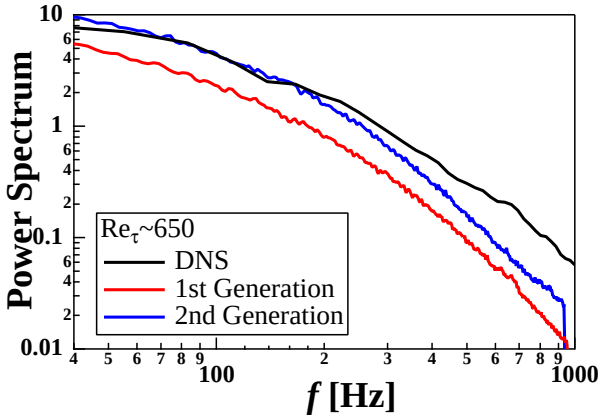

Fig. 11 Comparison of the power spectrum of wall shear stress between the present measurement data in turbulent channel flow and the DNS data [10].

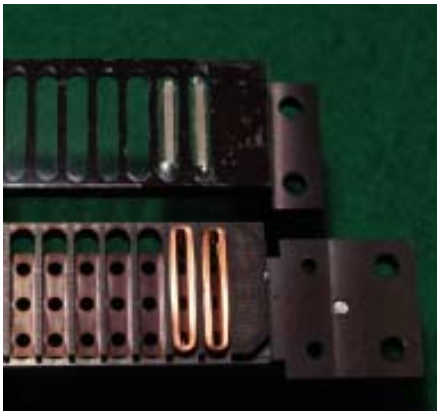

Fig. 12 Magnified view of arrayed wall-deformation magnetic actuator (2.4mm x 14.2 mm).

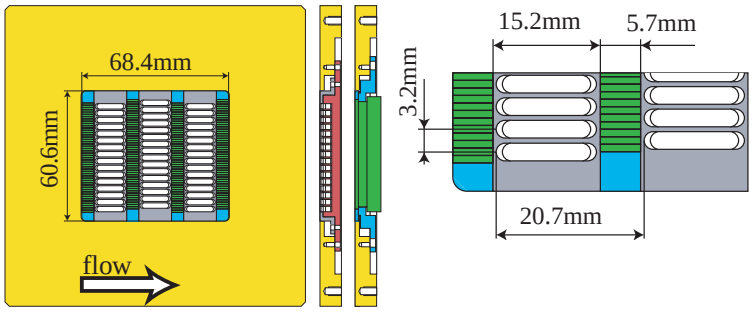

Fig. 13 The 2nd generation feedback control system with 192 sensors and 48 actuators.